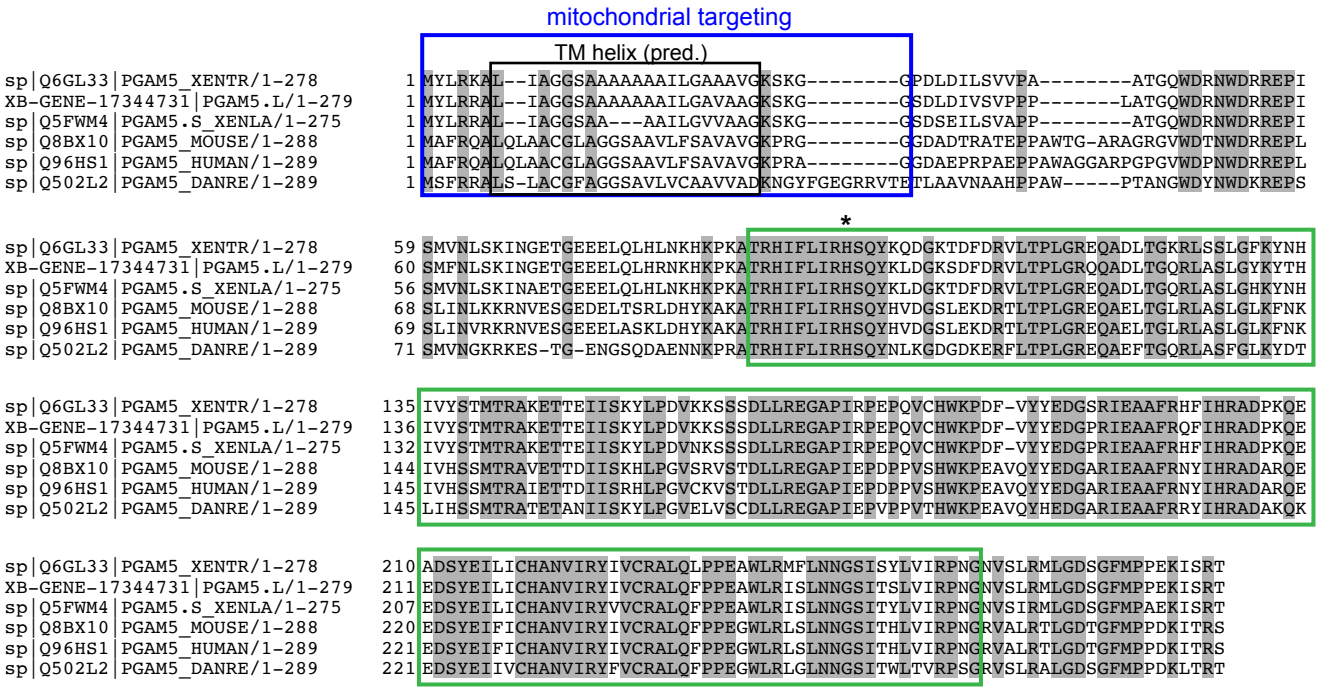

Supplementary Figure 1

Alignment of *Xenopus tropicalis* Pgam5, *Xenopus laevis* Pgam5.S and Pgam5.L to the zebrafish, human and mouse orthologs (Uniprot Accession Numbers *X. tropicalis* Pgam5 Q6GL33, *X. laevis* Pgam5.S Q5FWM4, *X. laevis* Pgam5 was translated from XB-GENE-17344731, *D. rerio* Pgam5 Q502L2, *H. sapiens* PGAM5 Q96HS1, *M. musculus* Pgam5 Q8BX10). Identical amino acids are shaded grey. The boxes mark functional features: blue – mitochondrial targeting sequence (Lo and Hannink, 2008), black: predicted transmembrane helix, green – PGAM domain. Histidine 105 (human numbering) in the catalytic center is labeled with an asterisk.

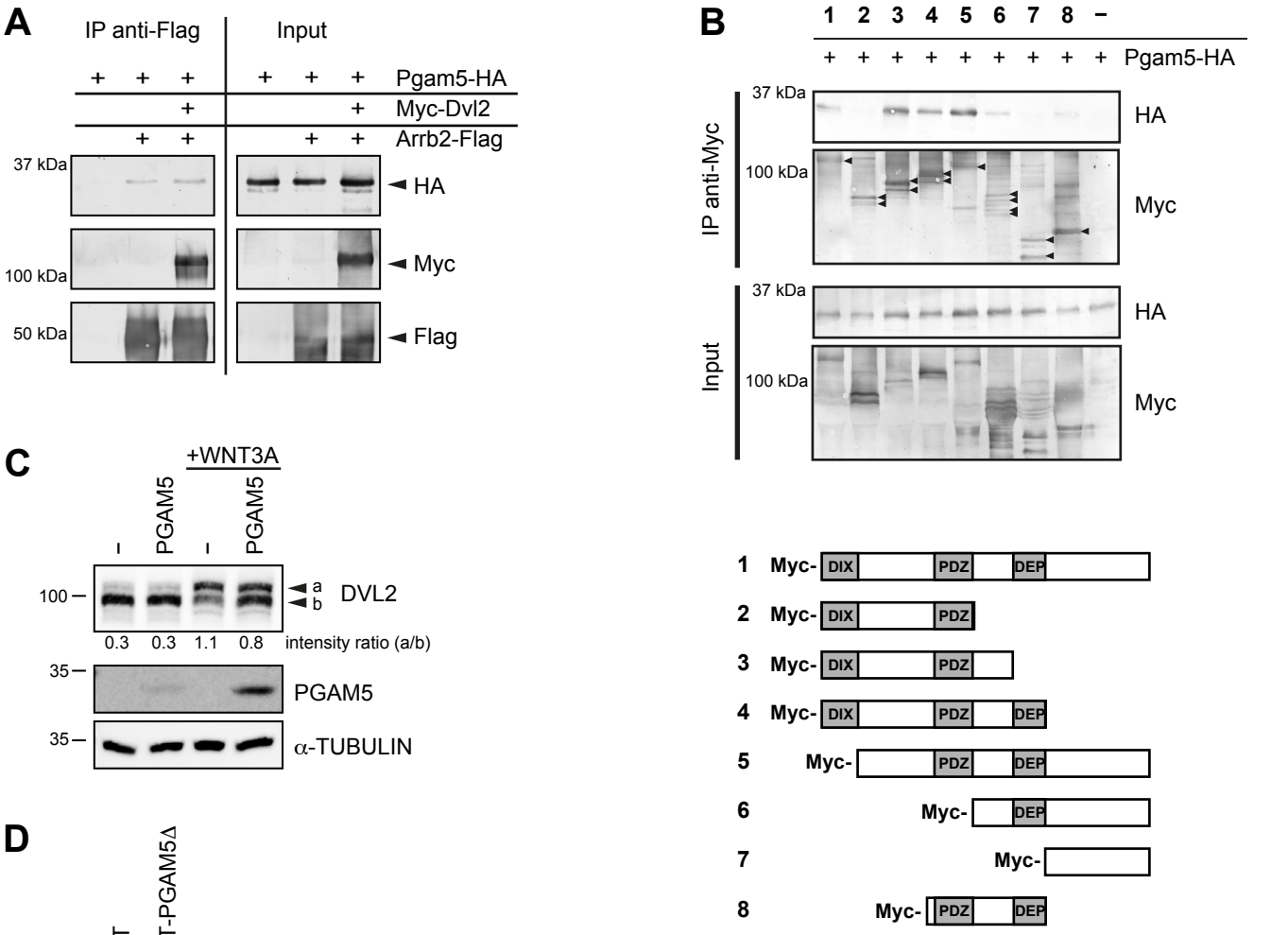

Supplementary Figure 2

(A) Co-immunoprecipitation of overexpressed proteins shows a weak interaction of Pgam5 with Arrb2, which is slightly increased by co-expression of Dvl2. (B) Western blot corresponding to Fig. 1D. The binding site of Pgam5 to Dvl2 was mapped to the region interspacing the PDZ and DEP domain of Dvl2 by co-immunoprecipitation of Pgam5-HA with a series of truncated Dvl2-Myc constructs (1-8) as illustrated.
(C) Overexpression of PGAM5 partially reverted WNT3A induced electrophoretic mobility shifts of endogenous DVL2 in HEK 293T cells, indicating that PGAM5 dephosphorylates DVL2. (D) HA-DVL2 was immunoprecipitated, washed with high stringency to remove bound proteins and incubated with recombinant GST, GST-PGAM5Δ (lacking the N-terminal mitochondrial targeting sequence) or Calf Intestinal Alkaline Phosphatase (CIP) for 30 min at 37°C. The sample incubated with GST showed two bands. After incubation with GST-PGAM5Δ or CIP only one band with higher electrophoretic mobility remained, which confirmed that DVL2 is directly dephosphorylated by PGAM5.

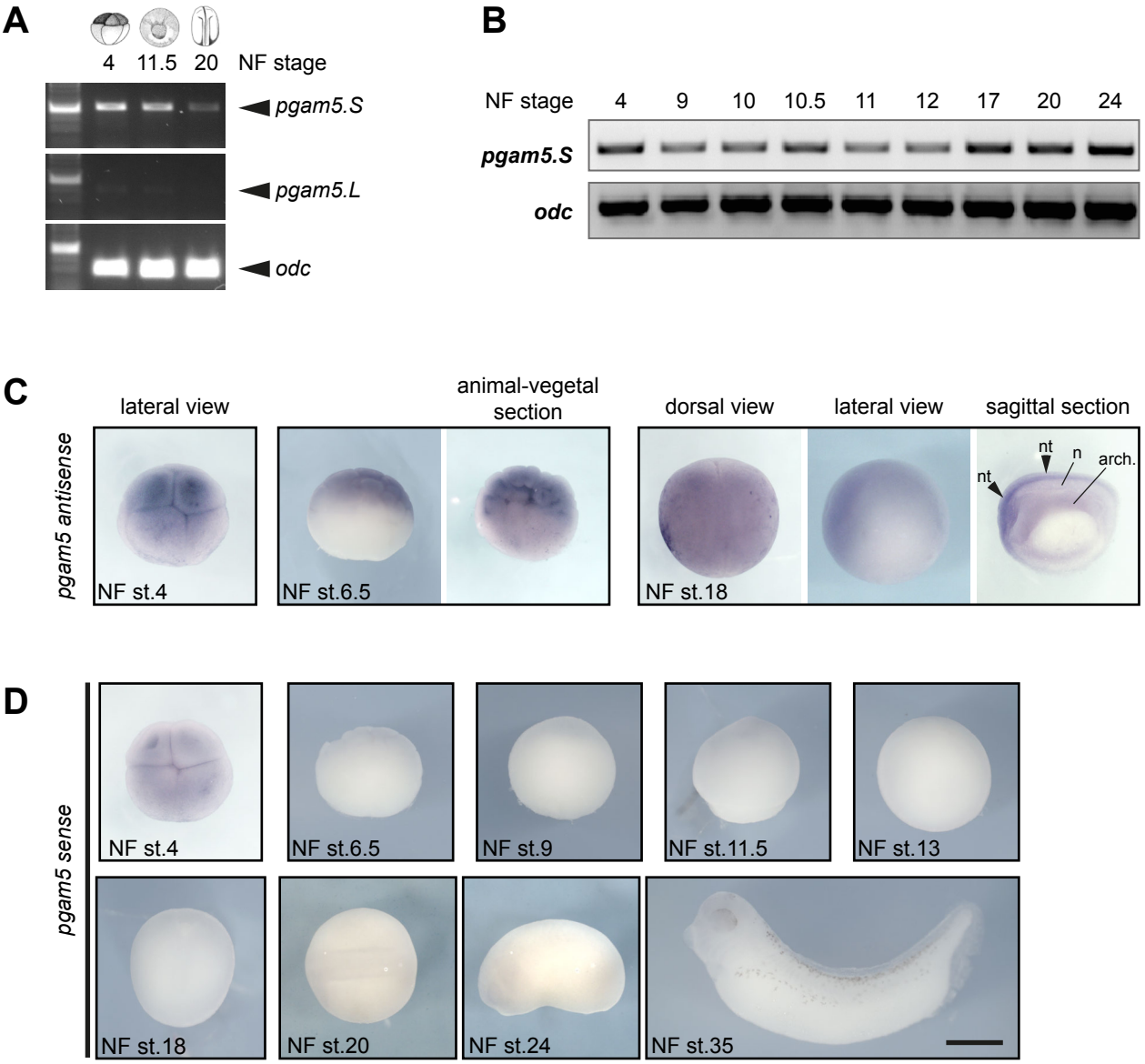

Supplementary Figure 3

(A) Transcripts of *pgam5*.S and *pgam5*.L homeologs were amplified by RT-PCR from whole embryos of the indica-ted stages; *ornithine decarboxylase* (*odc*) was used as house-keeping gene. The arrows indicate the expected fragment size. In contrast to *pgam5*.S, transcripts of *pgam5*.L were barely detectable and only in stage 4 embryos. (B) *pgam5*.S transcripts were present maternally (NF stage 4) and throughout early embryonic development (NF stages 9-24).

(C) Supplementary in situ hybridization data. Maternal *pgam5.S* transcripts were detected predominantly in the animal blastomeres at NF stage 4 (8-cell stage) and at early blastula stage 6.5. At stage 18/19 *pgam5* was broadly expressed in the dorsal ectoderm and the neural tube (nt). A sagittal section showed that expression was strongest in the anterior neural tube and gradually decreased towards posterior (arrowheads indicate neural tube (nt), n – notochord, arch. – archenteron). The archenteron cavity appears stained due to trapped dye.
(D) Sense controls corresponding to images in (A) and in Figure 3A.

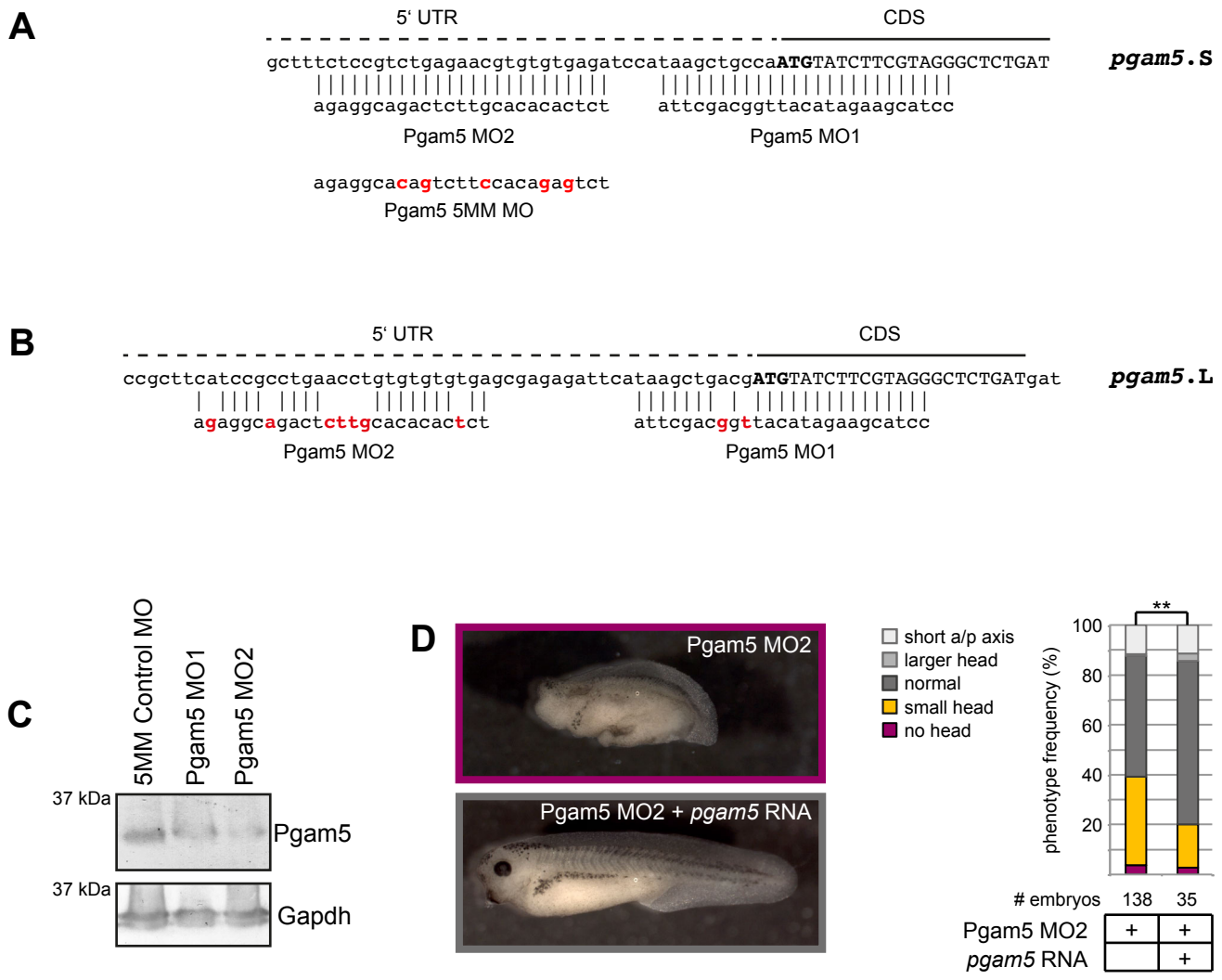

Supplementary Figure 4

(A) Translation-blocking antisense morpholino oligonucleotides were used to knock-down Pgam5 in *Xenopus laevis* embryos. Pgam5 MO1 and Pgam5 MO2 target two non-overlapping sites in *pgam5*.S transcripts at and close to the translation start respectively. The alignment shows the binding sites of MO1 and MO2 to the *pgam5*.S mRNA and base exchanges in the Pgam5 5-mismatch Control MO. (B) Alignment of Pgam5 MO1 and Pgam5 MO2 to *pgam5*.L. Pgam5 MO1 aligns with only two mismatches also to *pgam5*.L and therefore MO1 can be expected to suppress also translation from *pgam5*.L. The sequence in *pgam5*.L corresponding to the Pgam5 MO2 binding site contains seven nucleotide exchanges, therefore Pgam5 MO2 is not expected to affect *pgam5*.L translation. (C) Injection of either Pgam5 MO1 or Pgam5 MO2 into both blastomeres at the two-cell stage resulted in knock-down of Pgam5 at stage 11.5.

(D) Representative phenotypes of embryos injected with 0.4 pmol Pgam5 MO2 or co-injected with MO-insensitive *pgam5* RNA as indicated. Co-injection of *pgam5* RNA rescues the phenotype of Pgam5 morphant embryos. Frequencies of phenotypes from at least three independent experiments are summarized in the graph; the total numbers of embryos are provided below each column. The χ2-test was used for statistical analysis (** p-value < 0.01).

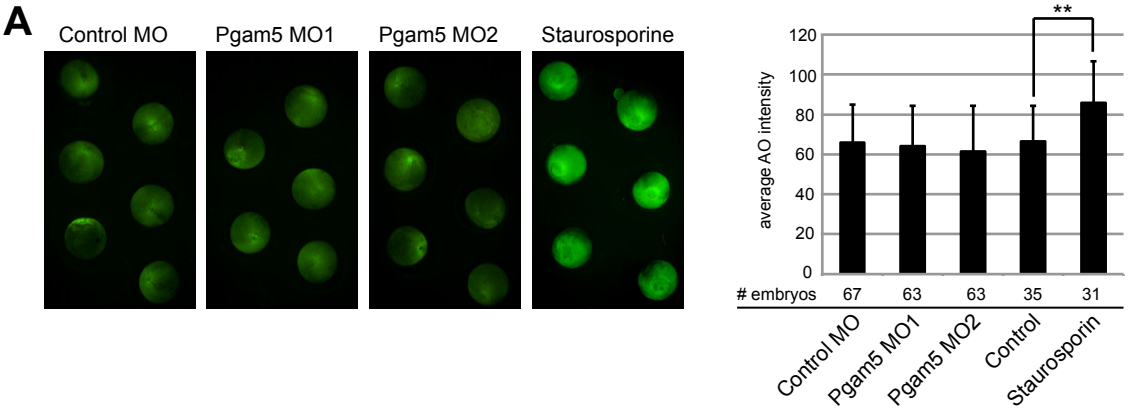

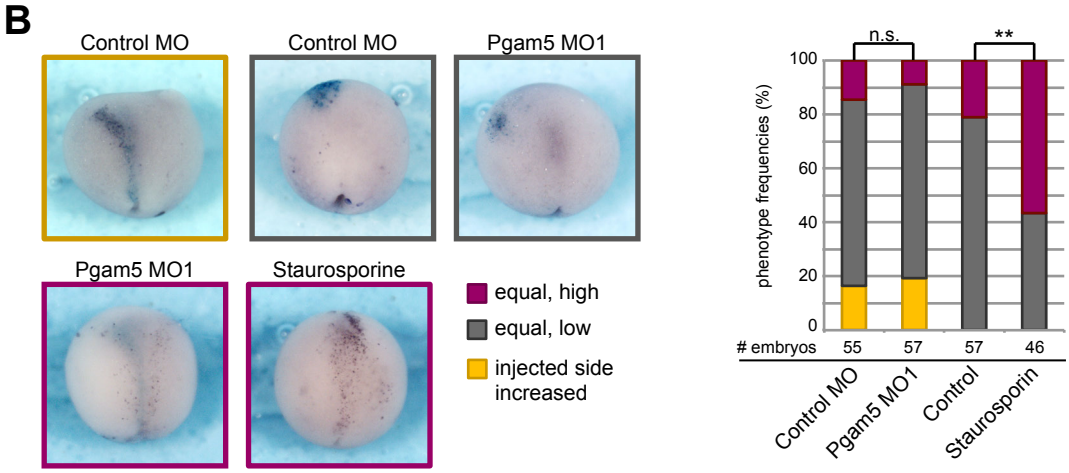

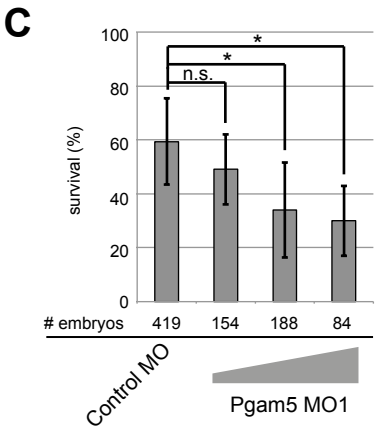

Supplementary Figure 5

Knock-down of Pgam5 did not cause increased cell death.

(A) Embryos were injected with 0.4 pmol Control MO, Pgam5 MO1 or Pgam5 MO2 into both blastomeres at the two-cell stage. At NF stage 12.5 embryos were stained for dead cells with 1 µg/ml Acridine Orange in 0.1x MBSH for 30 min, washed three times with 0.1x MBSH and imaged using a Leica M165FC stereomicroscope equipped with epifluorescence optics and a Jenoptik ProgRes C14 camera. As positive control, embryos were treated at NF stage 11.5 for 2h with 1µM staurosporine or buffer only, stained with Acridine Orange and imaged as described above. Image acquisition parameters were kept constant for all images. Mean fluorescence intensities were measured for each embryo using the Image J software package. The images show representative embryos injected with Control MO, Pgam5 MO1 or Pgam5 MO2 as well as staurosporine-treated embryos. The average fluorescence intensities ± SD are plotted in the graph; values did not differ significantly between Control MO, MO1 and MO2 (separate variances t-test, p-values > 0.7), staurosporine treatment significantly increased Acridine Orange fluorescence intensity compared to control embryos (** p-value < 0.01). The total numbers of analyzed embryos from four independent experiments are given below each column.

(B) Embryos were injected with 0.4 pmol Control MO or Pgam5 MO1 and co-injected with 100 pg pCS2 *LacZ* into one blastomere at the four-cell stage. As positive control, embryos were treated with 1µM staurosporine for 1h at NF stage 19. At NF stage 20 embryos were fixed and stained for β-Galactodidase. Cleaved Caspase 3 (Cleaved Casp3) was detected by whole-mount immunostaining and colorimetric Alkaline Phosphatase staining (NBT/BCIP). For MO-injected embryos Cleaved Casp3-positive cells on injected and uninjected sides were compared and categorized into equal (low/high) or increased numbers in the injected side. Staurosporine-treated embryos were compared with control embryos and categorized into low or high number of Cleaved Casp3-positive cells. The graph summarizes the results from four independent experiments (** p-value < 0.01 χ^2-test). The total numbers of embryos are provided below each column.

(C) Embryos were injected with 1.6 pmol Control MO or 0.4 pmol, 0.8 pmol or 1.6 pmol Pgam5 MO1 and cultured till NF stage 40. The graph shows the average survival rates from at least three independent experiments. The total numbers of embryos are provided below each column. Injection of 0.4 pmol MO1 did not significantly affect survival, whereas survival rates dropped significantly after injection of higher doses of MO1 (separate variances t-test, * p-value < 0.05).

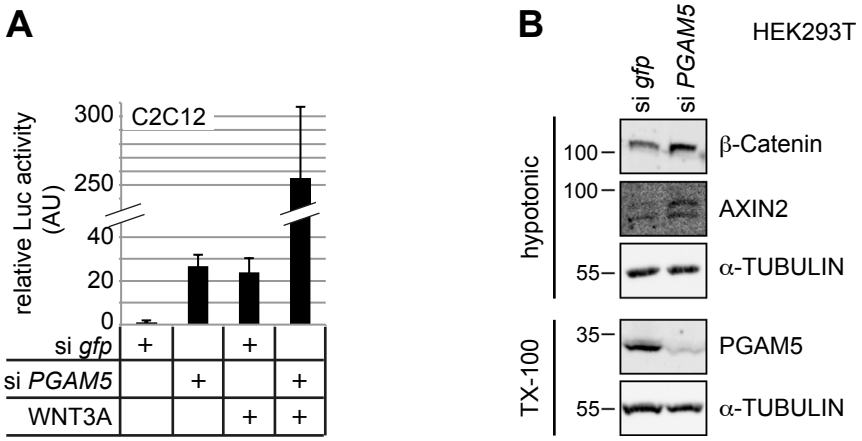

Supplementary Figure 6

(A) Knock-down of PGAM5 by siRNA transfection strongly enhanced responsiveness of murine C2C12 cells to WNT3A stimulation as determined by TOP-Flash reporter gene assays normalized to β-Galactosidase. (B) PGAM5 knock-down in HEK293T cells resulted in stabilization of cytoplasmic β-Catenin and upregulation of the feedback target AXIN2.

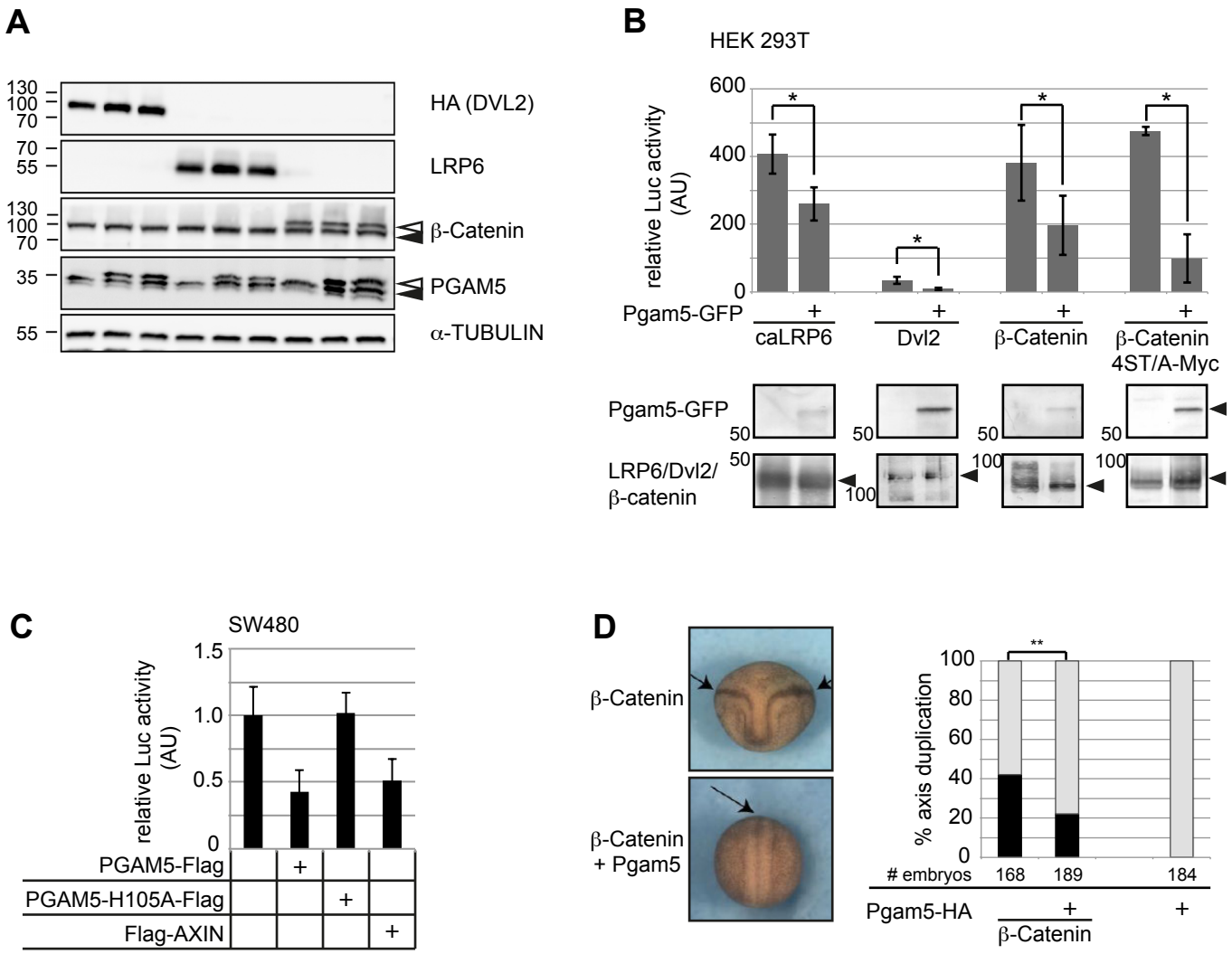

Supplementary Figure 7

(A) Expression of overexpressed proteins corresponding to Figure 7A was confirmed by Western Blot. Filled arrowheads indicate endogenous proteins, open arrowheads indicate overexpressed proteins. (B) *Xenopus* Pgam5 antagonized TOP-Flash activation by constitutively-active LRP6, Dvl2, β-Catenin or stabilized β-Catenin 4ST/A-Myc. The graph shows average ± SD from at least three independent experiments. Statistical significance of deviations was calculated using the t-test for the hypothesis of the mean (* p-value < 0.05). Expression of overexpressed proteins was confirmed by Western Blot; corresponding blots are provided below the respective columns. (C) Overexpression of PGAM5 in SW480 colon carcinoma cells suppressed constitutive Wnt/β-Catenin activity; the phosphatase-inactive mutant PGAM5-H105A had no effect. Overexpression of AXIN downregulated TOP-Flash activity comparable to PGAM5. TOP-Flash values were normalized to β-Galactosidase. (D) Secondary body axes were induced in *Xenopus laevis* embryos by injection of 400 pg *β-catenin* RNA and 100 pg *pgam5* RNA was co-injected as indicated into both ventral blastomeres at the four-cell stage. The graph shows the frequency of axis duplication from four independent experiments; statistical significance of deviations was calculated using the χ2-test; ** p-value < 0.01. Images show representative examples of embryos; arrows indicate neural tubes in the primary and – if present – in the secondary axis.

Supplementary Table 1

Plasmids and antisense Oligonucleotides

Plasmid / Morpholino / siRNA		**Reference**
Pgam5 MO1	5'-cctacgaagatacattggcagctta-3'	this study
Pgam5 MO2	5'-tctcacacacgttctcagacggaga-3'	this study
Pgam5 5MM MO	5'-tctgagacaccttctgacacggaga-3'	this study
si *PGAM5*	5'-cgcccgugucucauuggaa -3'	this study
si *gfp*	5´-gcuaccuguuccauggcca -3`	this study
pCRII Pgam5		this study
pCS2+ Pgam5-HA		this study
pCS2+ Pgam5-GFP		this study
pCS2+ PGAM5-Flag		this study
pCS2+ PGAM5-H105A-Flag		this study
pcDNA3.1 PGAM5-Flag		Takeda et al., 2009
pcDNA3.1 PGAM5-H105A-Flag		Takeda et al., 2009
pGEX4T3 PGAM5Δ		this study
pN1 PGAM5		this study
pCS2+ DKK1-GFP		Kagermeier-Schenk et al., 2011
pcDNA3.1 Arrb2-Flag		Seitz et al., 2014
pCS2+ myc-Dvl2		Seitz et al., 2014
pcDNA3.1 HA-DVL2		this study
pcDNA3.1 Flag-AXIN		Kishida et al., 1999
pCS2+ LRP6 ΔE1-E4		Mao et al., 2001
pCS2+ β-Catenin-myc		Yost et al., 1996
pCS2+ β-Catenin 4ST/A-myc		Yost et al., 1996
pcDNA3.1 beta-Catenin S33Y		this study
pCS2+ Tcf1-Flag		Ralph Rupp, Munich
pCS2+ LacZ		Schille et al., 2016
pGL3 Super 8x TOPFlash		Korinek et al., 1997
pGL TK Renilla		Promega GmbH, Mannheim, Germany

Supplementary Table 2

Antibodies and reagents

Antibody / Reagent	Dilution	Source / Reference
Rabbit anti-PGAM5	1:1000	Abcam plc, Cambridge, UK; # ab126534
Mouse anti-PGAM5	1:1000	Atlas Antibodies AB, Stockholm, Sweden #AMAb90803
Rabbit anti-DVL2	1:1000	Proteintech Europe Inc, Manchester, UK #12037-1-AP
Mouse anti-Dvl2	1:500	bio-techne, Minneapolis, USA; #MAB4216
Rabbit anti-ARRB2	1:1000	Proteintech Europe, Manchester, UK #10171-1-AP
Mouse anti-Arrb2	1:1000	Abcam plc, Cambridge, UK; #ab54790
Rabbit anti-β-Catenin	1:1000	Santa Cruz Biotechnology Inc., Dallas, TX, USA #sc-7199
Rat anti-β-Catenin	1:1000	Ralph Rupp, Ludwig-Maximilians-University Munich, Germany
Rabbit anti-GFP	1:1000	Cell Signaling Technology Inc., Danvers, MA, USA #2956
Rabbit anti-GFP	1:2000	Acris Antibodies GmbH, Herford, Germany; #SP3005P
Mouse anti-GAPDH	1:2000	Proteintech Europe Inc, Manchester, UK; #60004-1-Ig
Rabbit anti-TIMM44	1:500	Proteintech Europe Inc, Manchester, UK #13859-1-AP
Mouse anti-Lamin B2	1:500	Santa Cruz Biotechnology Inc., Dallas, TX, USA #sc-56147
Rabbit anti-panCadherin	1:1000	Cell Signaling Technology Inc., Danvers, MA, USA #4068
Mouse anti-dephospho-β-Catenin	1:500	Merck Millipore, Darmstadt, Germany; #05-665
Mouse anti-Axin2 (C/G7)	1:50	Lustig et al., 2002
Rat anti-α-Tubulin	1:1000	AbD Serotec; #MCA77G
Mouse anti-β-Actin	1:1000	Sigma-Aldrich Chemie GmbH, Munich, Germany; A5441

Rabbit anti-HA	1:1000	Sigma-Aldrich Chemie GmbH, Munich, Germany; H6908
Mouse anti-GST	1:1000	Sigma-Aldrich Chemie GmbH, Munich, Germany; G1160
Mouse anti-Flag immobilized	assay dependent	Sigma-Aldrich Chemie GmbH, Munich, Germany; #A2220
Dynabeads Protein G	assay dependent	ThermoFisher Germany, Darmstadt, Germany; #10004D
Staurosporine	1µM	Cell Signaling Technology Inc., Danvers, MA, USA #9953
Acridine Orange	1µg/ml	Applichem GmbH, Darmstadt, Germany; #A1398
Rabbit anti-Cleaved Caspase 3	1:500	Cell Signaling Technology Inc., Danvers, MA, USA; #9661

Supplementary Table 3

Primers for qRT-PCR and RT-PCR

Primer Name	Sequence	Reference
qRT-PCR		
odc fwd	cattgcagagcctgggagata	Schambony and Wedlich, 2007
odc rev	tccactttgctcattcaccataac	Schambony and Wedlich, 2007
xnr3 fwd	cgagtgcaagaaggtggaca	Bryja et al., 2007
xnr3 rev	atcttcatggggacacagga	Bryja et al., 2007
msgn1 fwd	ctggacaaggtctggaggagat	this study
msgn1 rev	tttatgcccatgatccttcttg	this study
hoxd1 fwd	ggacaaatttcaccaccaaaca	this study
hoxd1 rev	ggtatcgttgagctgcagagag	this study
dkk1 fwd	gatgcctacccgctctacagtt	this study
dkk1 rev	ggacacaaattccgttgctaca	this study
RT-PCR		
odc_fwd	gatgggctggatcgtatcgt	Schille et al., 2016
odc_rev	tggcagcagtacagacagca	Schille et al., 2016
pgam5.S_fwd1	atcccaagcaggaagaagacag	this study
pgam5.S_rev1	agcccaagaaataaggcacaga	this study
pgam5.S_fwd2	atctcagtgcagcggaaactc	this study
pgam5.S_rev2	tgctctcgtcattgtggagtaaa	this study
pgam5.L_fwd1	gacgtcagtgtggtggaaactc	this study
pgam5.L_rev1	actgtgagtgtcggatcaggaa	this study

Supplementary References

Bryja, V., Gradl, D., Schambony, A., Arenas, E. and Schulte, G. (2007). Beta-arrestin is a necessary component of Wnt/beta-catenin signaling in vitro and in vivo. *Proc Natl Acad Sci USA* **104**, 6690–6695.

Kagermeier-Schenk, B., Wehner, D., Ozhan-Kizil, G., Yamamoto, H., Li, J., Kirchner, K., Hoffmann, C., Stern, P., Kikuchi, A., Schambony, A., et al. (2011). Waif1/5T4 inhibits Wnt/β-catenin signaling and activates noncanonical Wnt pathways by modifying LRP6 subcellular localization. *Dev Cell* **21**, 1129–1143.

Kishida, S., Yamamoto, H., Hino, S., Ikeda, S., Kishida, M. and Kikuchi, A. (1999). DIX domains of Dvl and axin are necessary for protein interactions and their ability to regulate beta-catenin stability. *Mol Cell Biol* **19**, 4414–4422.

Korinek, V., Barker, N., Morin, P. J., van Wichen, D., de Weger, R., Kinzler, K. W., Vogelstein, B. and Clevers, H. (1997). Constitutive transcriptional activation by a beta-catenin-Tcf complex in APC-/- colon carcinoma. *Science* **275**, 1784–1787.

Lustig, B., Jerchow, B., Sachs, M., Weiler, S., Pietsch, T., Karsten, U., van de Wetering, M., Clevers, H., Schlag, P. M., Birchmeier, W., et al. (2002). Negative feedback loop of Wnt signaling through upregulation of conductin/axin2 in colorectal and liver tumors. *Mol Cell Biol* **22**, 1184–1193.

Mao, J., Wang, J., Liu, B., Pan, W., Farr, G. H., Flynn, C., Yuan, H., Takada, S., Kimelman, D., Li, L., et al. (2001). Low-density lipoprotein receptor-related protein-5 binds to Axin and regulates the canonical Wnt signaling pathway. *Mol Cell* **7**, 801–809.

Schambony, A. and Wedlich, D. (2007). Wnt-5A/Ror2 regulate expression of XPAPC through an alternative noncanonical signaling pathway. *Dev Cell* **12**, 779–792.

Schille, C., Bayerlová, M., Bleckmann, A. and Schambony, A. (2016). Ror2 signaling is required for local upregulation of GFD6 and activation of BMP signaling at the neural plate border. *Development* **143**, 3182–3194.

Seitz, K., Dürsch, V., Harnoš, J., Bryja, V., Gentzel, M. and Schambony, A. (2014). β-Arrestin interacts with the beta/gamma subunits of trimeric G-proteins and dishevelled in the Wnt/Ca(2+) pathway in xenopus gastrulation. *PLoS ONE* **9**, e87132.

Takeda, K., Komuro, Y., Hayakawa, T., Oguchi, H., Ishida, Y., Murakami, S., Noguchi, T., Kinoshita, H., Sekine, Y., Iemura, S.-I., et al. (2009). Mitochondrial phosphoglycerate mutase 5 uses alternate catalytic activity as a protein serine/threonine phosphatase to activate ASK1. *Proc Natl Acad Sci USA* **106**, 12301–12305.

Yost, C., Torres, M., Miller, J. R., Huang, E., Kimelman, D. and Moon, R. T. (1996). The axis-inducing activity, stability, and subcellular distribution of beta-catenin is regulated in Xenopus embryos by glycogen synthase kinase 3. *Genes Dev* **10**, 1443–1454.